Applied Catalysis B: Environmental 84 (2008) 835–842

Contents lists available at ScienceDirect

Applied Catalysis B: Environmental

journal homepage: www.elsevier.com/locate/apcatb

# Photocatalytic reduction of $Ag_2SO_4$ by the Dawson anion $\alpha$-$[P_2W_{18}O_{62}]^{6-}$ and tetracobalt sandwich complexes

Claire Costa-Coquelard, Delphine Schaming, Isabelle Lampre *, Laurent Ruhlmann **

*Laboratoire de Chimie Physique, UMR 8000 CNRS/Université Paris-Sud 11, Faculté des Sciences d'Orsay, Bâtiment 349, 91405 Orsay Cedex, France*

ARTICLE INFO

*Article history:*
Received 23 April 2008
Received in revised form 16 June 2008
Accepted 18 June 2008
Available online 26 June 2008

*Keywords:*
Dawson
Polyoxometalates
Photocatalysis
Silver

ABSTRACT

The photocatalytic behaviours of the Dawson salt $\alpha$-$K_6[P_2W_{18}O_{62}]$ and two isomers of the tetracobalt Dawson-derived sandwich complexes, $\alpha\beta\beta\alpha$-$Na_{17}[Co_4(H_2O)(OH)(P_2W_{15}O_{56})_2]\cdot 51H_2O\cdot 2NaCl$ and $\alpha\alpha\beta\alpha$-$Na_{16}[Co_4(H_2O)_2(P_2W_{15}O_{56})_2]\cdot 51H_2O$ (abbreviated $\beta\beta$-$\{Co_4P_4W_{30}\}$ and $\alpha\beta$-$\{Co_4P_4W_{30}\}$, respectively), are described and compared.

The direct photochemical excitation of the polyoxometalates (POM) in the presence of propan-2-ol as electron donor leads to their reduction. With polyoxometalates as photocatalyst and propan-2-ol as sacrificial electron donor, the reduction of $Ag^I{}_2SO_4$ from aqueous solutions is observed leading to metallic $Ag_n{}^0$ clusters and colloidal metal nanoparticles stabilized by POM.

In the case of both $\{Co_4P_4W_{30}\}$, TEM experiments reveal that most of the $Ag_n$ particles obtained with a slight excess of $Ag^+$ are spherical with a quite large distribution in size between 10 and 100 nm.



## 1. Introduction

Polyoxometalates (POM) are well-defined metal-oxygen cluster anions constituted of early metal elements in their highest oxidation state with a wide variety of structures and properties. They can exchange several electrons while their structure remains intact. The ability to modify their redox and chemical properties by replacing one or many elements, renders them particularly attractive for catalytic, electrocatalytic and also photocatalytic applications [1–3].

Recently, Papaconstantinou and co-workers reported that photocatalytical processes using POM can be used as an alternative solution for recovery of metals or synthesis of metal nanoparticles [4–11]. They showed that photochemically reduced $[SiW_{12}O_{40}]^{4-}$ or $[PW_{12}O_{40}]^{3-}$ Keggin anions as well as $[P_2Mo_{18}O_{62}]^{6-}$ Dawson anion in the presence of metal ions, such as $Ag^+$, $AuCl_4^-$, $Pd^{2+}$ and $PtCl_6^{2-}$, lead to the formation of metal nanoparticles capped by the Keggin or Dawson anions. The photochemically reduced POM were produced by illumination in the O–M charge transfer band situated in the UV/near visible spectral domain in the presence of an organic electron donor. Indeed, the excited POM are strong oxidants able to abstract electrons from organic compounds, for instance propan-2-ol [12–14]. So, POM serve both as photocatalysts in the electron transfer from organic substrates to metal ions and play also a stabilizer role, since the obtained metal colloids are stable against aggregation [6].

At natural pH, $[SiW_{12}O_{40}]^{4-}$, $[PW_{12}O_{40}]^{3-}$ Keggin anions as well as $[P_2Mo_{18}O_{62}]^{6-}$ Dawson anion exchange one-electron by redox process. It appears interesting to study the influence of the number of exchanged electrons, the charge and the size of the polyoxometalate on the photocatalytic efficiency for the reduction of metal cations as well as the stabilization of nanoparticles and their diameters.

Within this context, we have undertaken a study on the photocatalytic properties of sandwich tungstophosphate Dawson type polyanions. We report here the photocatalytic reduction of silver cations in aqueous solutions in the presence of propan-2-ol using the Dawson salt, $\alpha$-$K_6[P_2W_{18}O_{62}]$, and two isomers of the tetracobalt Dawson-derived sandwich complexes, namely $\alpha\beta\beta\alpha$-$Na_{17}[Co_4(H_2O)(OH)(P_2W_{15}O_{56})_2]\cdot 51H_2O\cdot 2NaCl$ and $\alpha\alpha\beta\alpha$-$Na_{16}[Co_4(H_2O)_2(P_2W_{15}O_{56})_2]\cdot 51H_2O$ (abbreviated $\beta\beta$-$\{Co_4P_4W_{30}\}$ and $\alpha\beta$-$\{Co_4P_4W_{30}\}$, respectively) (Fig. 1). Let us recall that the $\beta$ junction implies a connection between one $WO_6$ (or $MO_6$) and a dimetallic unit $W_2O_{10}$ (or $M_2O_{10}$) whereas the $\alpha$ junction is defined as a bis-$\mu$-oxo connection between one $WO_6$ (or $MO_6$) and two dimeric units $W_2O_{10}$ (or $M_2O_{10}$); alternately the $\alpha$ junction may be described by a group of three mutually corner-coupled $WO_6$ (or $MO_6$) octahedrons (Fig. 1, right) [15].

* Corresponding author. Tel.: +33 1 69 15 45 11; fax: +33 1 69 15 61 88.
** Corresponding author. Tel.: +33 1 69 15 47 32; fax: +33 1 69 15 61 88.
*E-mail addresses:* isabelle.lampre@lcp.u-psud.fr (I. Lampre), laurent.ruhlmann@lcp.u-psud.fr (L. Ruhlmann).

0926-3373/$ – see front matter © 2008 Elsevier B.V. All rights reserved.
doi:10.1016/j.apcatb.2008.06.018

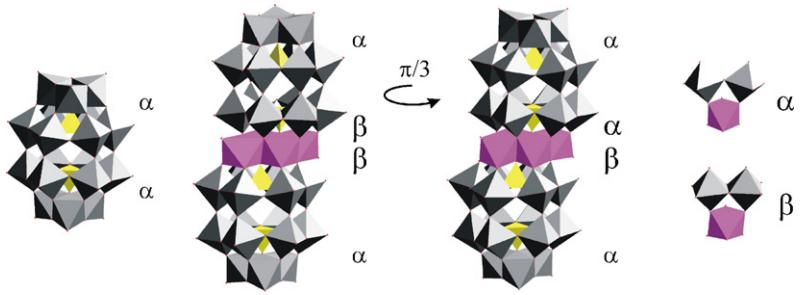


**Fig. 1.** Polyhedral representation of the studied POM: the Dawson anion α-$[P_2W_{18}O_{62}]^{6-}$, the two isomers of the tetracobalt Dawson-derived sandwich complexes, ββ-$\{Co_4P_4W_{30}\}$ and αβ-$\{Co_4P_4W_{30}\}$; and polyhedral representation of the α and β junctions.

The photoreduction capacity of the sandwich complexes is compared to that of the Dawson precursor α-$K_6[P_2W_{18}O_{62}]$ as the number of exchanged electrons can be increased due to the presence of two $\{P_2W_{15}\}$ moieties [16]. The influence of the symmetry of the sandwich complexes is also studied and the shape and stability of the obtained silver nanoparticles are characterised.

## 2. Experimental part

Most common laboratory chemicals were reagent grade, purchased from commercial sources and used without further purification. Water was obtained by passing through a Milli-$RO_4$ unit and subsequently through a Millipore Q water purification set.

The Dawson heteropolytungstate potassium salt, α-$K_6P_2W_{18}O_{62}$, was prepared by published method [17]. The two isomers of the tetranuclear Cobalt Dawson-derived sandwich complex, αββα-$Na_{17}[Co_4(H_2O)(OH)(P_2W_{15}O_{56})_2]\cdot 51H_2O\cdot 2NaCl$ and αααβ-$Na_{16}[Co_4(H_2O)_2(P_2W_{15}O_{56})_2]\cdot 51H_2O$, were prepared as described previously. The synthesis in neutral solution gives a mixture of symmetrical and unsymmetrical complexes in the proportions of 38 and 62%, respectively, while in acidic medium, only the symmetric complex is formed [16]. Pure unsymmetrical complex is obtained from the unsaturated tricobalt sandwich complex with addition of a slight excess of $Co^{2+}$ [18].

Irradiation was performed using a 300-W Xe arc lamp equipped with a water cell filter to absorb the near-IR radiation. According to the supplier, the irradiance of the lamp from 320 to 790 nm was around 50 mW $m^{-2}$ $nm^{-1}$. The samples consisted of 4 mL of aqueous solutions with propan-2-ol, POM and, if present, $Ag_2SO_4$, contained in a spectrophotometer quartz cell of 1 cm path length. Deaerated solutions were obtained by bubbling with Argon (Ar–U, from Air Liquide) before illumination. All the aqueous samples were at natural pH (initially 5.5) and all experiments were carried out at room temperature. We checked that the temperature of the solution did not increase by more than 2 degrees during light illumination.

UV–vis absorption spectra were recorded with a single beam Hewlett-Packard HP 8453 diode array spectrophotometer operated at a resolution of 2 nm.

Transmission electronic microscopy (TEM) observations were performed with a JEOL 100 CXII TEM instrument operated at an accelerating voltage of 100 kV. Samples for TEM analysis were prepared by solution drops deposited and dried on carbon-coated copper TEM grids.

## 3. Results and discussion

### 3.1. Photoreduction of the heteropolytungstate anions

It is well known that POM can be reduced to heteropoly-blue species in the presence of an organic compound as electron donor by UV illumination in the oxygen-to-metal charge transfer bands [19]. Fig. 2 shows the change in the optical absorption spectrum of a deaerated aqueous solution containing $2.5 \times 10^{-5}$ mol $L^{-1}$ α-$K_6[P_2W_{18}O_{62}]$ and 0.13 mol $L^{-1}$ propan-2-ol under UV illumination as well as the time evolution of the absorbance at two different wavelengths. α-$[P_2W_{18}O_{62}]^{6-}$ is spectrally characterised by oxygen-to-tungsten charge transfer (O–W CT) bands in the UV spectral domain ($\lambda < 380$ nm) and no absorption in the visible. In contrast, the reduced forms exhibit intense broad absorption bands around 600–700 nm attributed to *d–d* transitions and tungsten-to-tungsten charge transfer ($W^{5+}$–$W^{6+}$ CT) and the reduced forms also present a decrease in the O–W CT bands (Fig. 2A). The visible bands are responsible of the blue colouring of the solution upon illumination. The shift to shorter wavelengths of

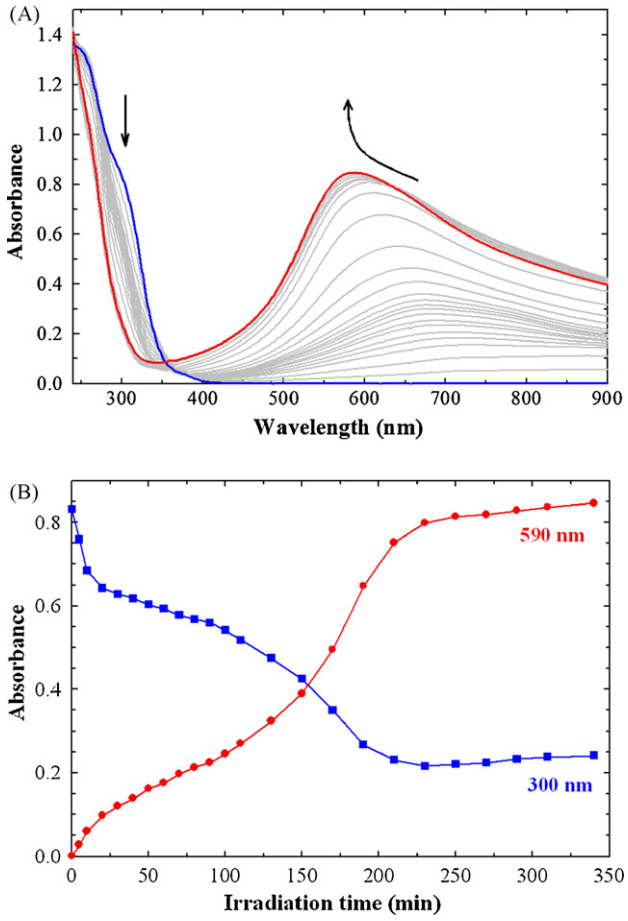


**Fig. 2.** (A) Change in the UV–vis absorption spectrum and (B) temporal evolution of the absorbance at two different wavelengths of a deaerated aqueous solution containing $2.5 \times 10^{-5}$ mol $L^{-1}$ α-$K_6[P_2W_{18}O_{62}]$ and 0.13 mol $L^{-1}$ propan-2-ol under illumination.

the visible absorption band maximum (from above 900 down to 587 nm) and the kinetic profiles at two wavelengths (Fig. 2B) clearly indicate the gradual reduction of α-$[P_2W_{18}O_{62}]^{6-}$. Given the spectral data reported by Papaconstantinou and Pope [20], it seems that the one- ($\lambda_{max}$ = 909 nm) to six-electron ($\lambda_{max}$ = 585 nm) reduced products are successively obtained during the 6 h of light exposure. At the end of the irradiation, we estimate a molar extinction coefficient around 35,600 $dm^3\ mol^{-1}\ cm^{-1}$, one-third higher than the reported value (23,800 $dm^3\ mol^{-1}\ cm^{-1}$ at 585 nm for α-$[H_4P_2W_{18}O_{62}]^{8-}$). However, Papaconstantinou and Pope worked with solutions of POM at pH 1.4 in which all the four- and six-electron reduced POM are protonated, what is maybe not the case in our experimental conditions. We did not measure the final pH of the solution but, given the initial concentration of α-$[P_2W_{18}O_{62}]^{6-}$, the total reduction to six electrons would lead to the formation of $1.5 \times 10^{-4}$ mol $L^{-1}$ protons, what would correspond to pH 3.8.

When the illumination is stopped, the absorption spectrum remains identical for more than 20 h showing the stability of the reduced products in anaerobic conditions. But, if the cell is open to air, the blue colour of the solution disappears in few hours and the initial spectrum of α-$[P_2W_{18}O_{62}]^{6-}$ is recovered indicating the total oxidation of the reduced forms by dioxygen.

The catalytic photooxidation of alcohols to aldehydes or ketones by heteropoly compounds has already been reported by several groups [12,14,21,22]. According to these studies, the mechanism for the first two reduction steps may be written as follows [19]:

$$\alpha\text{-}[P_2W_{18}O_{62}]^{n-} + (CH_3)_2CHOH \xrightarrow{h\nu} \alpha\text{-}[P_2W_{18}O_{62}]^{(n+1)-} + (CH_3)_2C^{\bullet}OH + H^+ \quad (1)$$

$$\alpha\text{-}[P_2W_{18}O_{62}]^{(n+1)-} + (CH_3)_2C^{\bullet}OH \rightarrow \alpha\text{-}[P_2W_{18}O_{62}]^{(n+2)-} + (CH_3)_2CO + H^+ \quad (2)$$

$$\alpha\text{-}[P_2W_{18}O_{62}]^{n-} + (CH_3)_2C^{\bullet}OH \rightarrow \alpha\text{-}[P_2W_{18}O_{62}]^{(n+1)-} + (CH_3)_2CO + H^+ \quad (3)$$

$$\alpha\text{-}[P_2W_{18}O_{62}]^{n-} + \alpha\text{-}[P_2W_{18}O_{62}]^{(n+2)-} \rightarrow 2\alpha\text{-}[P_2W_{18}O_{62}]^{(n+1)-} \quad (4)$$

with $n$ = 6 or 7.

In our experimental conditions (initial pH below 6 and decreasing as reduction occurs by formation of $H^+$), the subsequent reduction steps may be accompanied by protonations.

It is to be noted that precomplexation of alcohol and heteropolytungstate before photoactivation is possible as reported by Fox et al. [23] and, in that case, the photoinduced oxidation of alcohol could occur via a rapid two-electron transfer within the complex.

It has been reported [13] that, generally, the photochemical reactions proceed until the redox potential of the reduced polyoxometalate, here α-$[P_2W_{18}O_{62}]^{10-}$, is negative enough to reduce $H^+$. The fact that the absorption spectrum remains constant after switching off the illumination indicates that gradual reoxidation of reduced POM by $H^+$ is negligible in our experimental conditions. In contrast, in the presence of dioxygen, reoxidation of the reduced heteropolyanions is fast and effective even for the one-electron reduced species since the initial spectrum of the non-reduced α-$[P_2W_{18}O_{62}]^{6-}$ is recovered. That is in agreement with the previous study by Hiskia and Papaconstantinou [24].

Fig. 3 presents the optical absorption spectra of deaerated aqueous solutions containing $8 \times 10^{-6}$ mol $L^{-1}$ αββα-$Na_{17}[Co_4(H_2O)(OH)(P_2W_{15}O_{56})_2]\cdot 51H_2O\cdot 2NaCl$ or ααβα-$Na_{16}[Co_4$

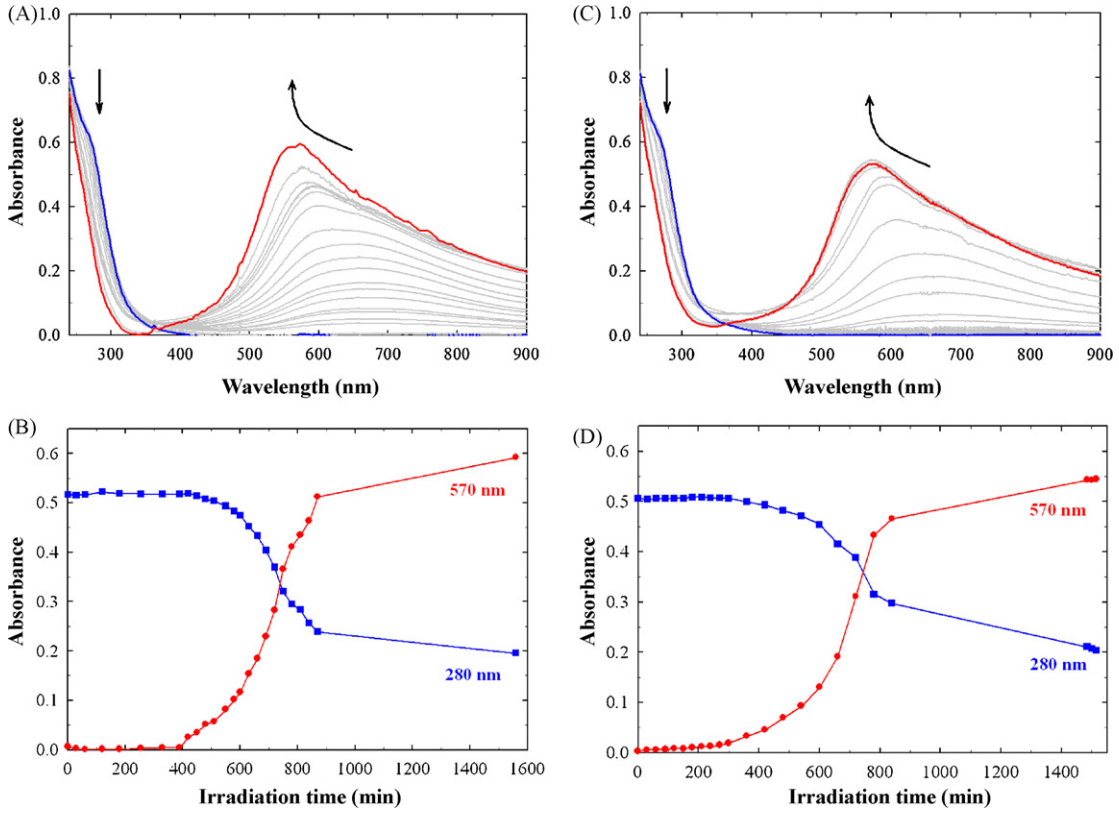


**Fig. 3.** (A and C) Change in the UV–vis absorption spectrum and (B and D) temporal evolution of the absorbance at two different wavelengths of deaerated aqueous solutions containing $8 \times 10^{-6}$ mol $L^{-1}$ αββα-$Na_{17}[Co_4(H_2O)(OH)(P_2W_{15}O_{56})_2]\cdot 51H_2O\cdot 2NaCl$ (A and B) or ααβα-$Na_{16}[Co_4(H_2O)_2(P_2W_{15}O_{56})_2]\cdot 51H_2O$ (C and D) and 0.13 mol $L^{-1}$ propan-2-ol under illumination.

$(H_2O)_2(P_2W_{15}O_{56})_2]\cdot 51H_2O$ and 0.13 mol $L^{-1}$ propan-2-ol. Under UV light exposure for several hours, while the O–W CT band of the POM below 320 nm decreases slightly, a new band around 570 nm appears and grows leading to a blue coloration of the solution. If the solution is put into contact with dioxygen, by opening the cell to air, the blue colour disappears and the initial spectrum of the solution before illumination is recovered. As just described for α-$[P_2W_{18}O_{62}]^{6-}$, such evolution is characteristic of the photolytic production of reduced POM in deaerated solution containing POM and propan-2-ol. The change in the shape and the blue shift of the visible absorption band indicate multielectron reduction. But, as no spectrochemical data are available for these compounds, it is not possible to determine the final degree of reduction. Electrochemical studies have shown that such compounds exhibit three successive reduction processes involving the W centres and related to four electrons; so, they can accept up to twelve electrons without decomposition. Consequently, as the first redox couple of the studied Dawson-derived sandwich polyoxometalates $\{Co_4P_4W_{30}\}$ is related to a four-electron reaction process [16], the mechanism should involve the photochemical oxidation of propan-2-ol by the excited POM and lead to the concomitant formation of the reduced POM($4e^-$) according to the global reaction:

$$\{Co_4P_4W_{30}\} + 2(CH_3)_2CHOH \xrightarrow{h\nu} \{Co_4P_4W_{30}\}^{4-} + 2(CH_3)_2CO + 4H^+ \quad (5)$$

It is to be noted that for the two $\{Co_4P_4W_{30}\}$ isomers having identical absorption spectra and similar redox potentials for the first reduction wave ($E^\circ$(POM/$POM^{4-}$) = −0.196 and −0.227 V vs. NHE at pH 3.5 for ββ-$\{Co_4P_4W_{30}\}$ and αβ-$\{Co_4P_4W_{30}\}$, respectively [18]), the photoreduction rate is found similar. So, no influence of the POM structure on the intermediate steps of reduction involving H-abstraction and/or electron transfer, as well as on possible precomplexation with alcohol, is observed.

### 3.2. Photoreduction of silver ions by heteropolytungstate anions

Whatever the studied POM, the addition of silver ions to aqueous solutions of POM induces an increase (of around 10 and 20% for α-$[P_2W_{18}O_{62}]^{6-}$ and both $\{Co_4P_4W_{30}\}$, respectively) in the absorbance of the O–W CT band (inset in Fig. 4A). Such change reveals interactions between silver cations $Ag^+$ and heteropolyanions attributed to electrostatic associations. Indeed, ion pairing between cations and POM anions has already been reported [25].

#### 3.2.1. Photoreduction in the absence of dioxygen

Illumination of deaerated aqueous solution containing $8 \times 10^{-6}$ mol $L^{-1}$ α-$K_6[P_2W_{18}O_{62}]$, 0.13 mol $L^{-1}$ propan-2-ol and $6.4 \times 10^{-5}$ mol $L^{-1}$ $Ag_2SO_4$ leads to the formation of silver nanoparticles (Fig. 4). Upon illumination, first the well-know plasmon absorption band of silver clusters around 400 nm is observed indicating that the $Ag^+$ cations are reduced and that metal atoms coalesce to form clusters stabilized by POM. Then, the absorption band of the reduced POM appears around 550–600 nm (Fig. 4A). After 450 min of light exposure, no change of the UV–vis spectra is noticed, indicating the end of the reactions and the total reduction of $Ag^+$ into $Ag_n$ clusters. The obtained plasmon band is very sharp and symmetric with a final absorbance greater than 2. Experiments performed with less concentrated solutions allowed us to evaluate the molar extinction coefficient per $Ag^0$ atom at the peak maximum to be around 21,800 $dm^3$ $mol^{-1}$ $cm^{-1}$. That characterizes very small spherical nanoparticles with an homogeneous size distribution [26–28]. The small size of the particles is corroborated by the fact the nanoparticles are not stable, the plasmon band disappearing when the illumination is stopped. As

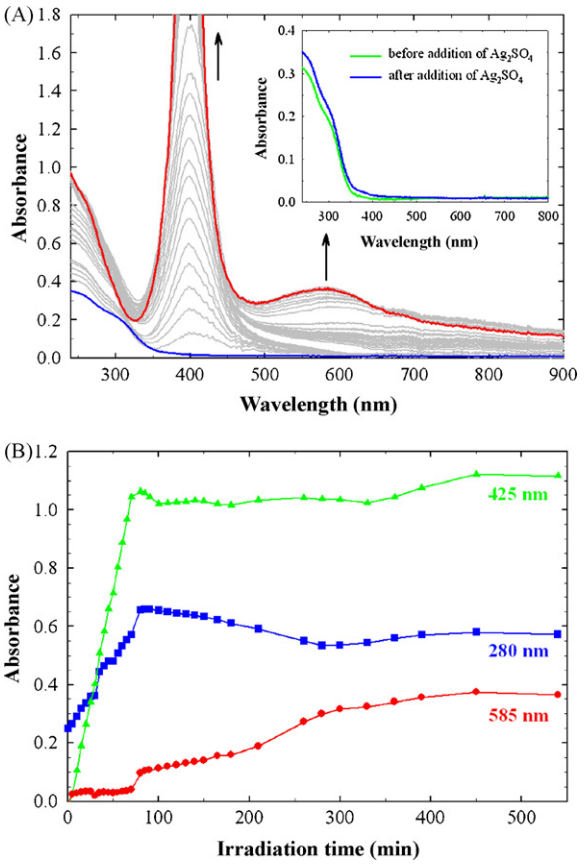


**Fig. 4.** (A) Change in the UV–vis absorption spectrum and (B) temporal evolution of the absorbance at three different wavelengths of a deaerated aqueous solution containing $8 \times 10^{-6}$ mol $L^{-1}$ α-$K_6[P_2W_{18}O_{62}]$, $6.4 \times 10^{-5}$ mol $L^{-1}$ $Ag_2SO_4$ and 0.13 mol $L^{-1}$ propan-2-ol under illumination. Inset in (A) UV–vis absorption spectra of the initial solution of α-$[P_2W_{18}O_{62}]^{6-}$ before and after addition of $Ag_2SO_4$.

neither band broadening nor light scattering is observed in the absorption spectrum, that decrease is not due to coalescence and precipitation but indicates reoxidation of the nanoparticles. Indeed, if the sample is illuminated again, the plasmon band reappears.

The plots of the time evolution of the absorbencies at characteristic wavelengths allow us to follow the successive formation of silver clusters and reduced POM (Fig. 4B). The absorbencies at 425 and 280 nm increase during the first 80 min of illumination while the absorbance at 585 nm remains constant and negligible. Then, the absorbance at 585 nm rises and progressively increases to reach a plateau after 450 min of illumination whereas the absorbance at 280 nm decreases for 200 min, slightly increases to also reach a constant value; for the meantime from 80 till 300 min of illumination, the absorbance at 425 nm remains roughly constant, then it presents a small increase and becomes constant after 450 min of illumination. These kinetic profiles show that the reduction of $Ag^+$ occurs at the beginning of the illumination and must be complete in 80 min since reduced POM are observed only after 80 min of illumination. We can estimate the rate of silver reduction to be $1.6 \times 10^{-6}$ mol $L^{-1}$ $min^{-1}$. That value is one order of magnitude lower than that reported by Troupis et al. [7] in the case of the photocatalytic reduction of silver by $[SiW_{12}O_{40}]^{4-}$ in the presence of 0.5 mol $L^{-1}$ propan-2-ol, for a similar ratio $Ag^+$/POM but concentrations 15 times higher than ours.

Those results give evidence that the α-$[P_2W_{18}O_{62}]^{6-}$ Dawson polyoxometalate exhibits a photocatalytic activity toward the

reduction of $Ag^+$ ions in the presence of propan-2-ol. As the reduction occurs immediately without induction time or initial apparition of reduced POM, we may assume that the initial reduction mechanism should proceed from the first reduced forms of POM (one or two electron(s)). However, whatever the reduction degree of the POM, the thermodynamics of the involved species are not favourable as the redox potentials of the POM couples, ($\alpha$-$[P_2W_{18}O_{62}]^{6-}$/$\alpha$-$[P_2W_{18}O_{62}]^{7-}$) to ($\alpha$-$[P_2W_{18}O_{62}]^{11-}$/$\alpha$-$[P_2W_{18}O_{62}]^{12-}$), are 0.30 V down to −0.86 V vs. NHE, respectively [29], and, the potential of the ($Ag^+/Ag^0$) couple is −1.75 V vs. NHE [30]. Consequently, we may suggest two explanations for the reduction of $Ag^+$ ions. On the one hand, we invoke the possible formation of a complex between the $Ag^+$ cations and the POM anions, leading to a change in the redox potentials. In fact, within association, the electric field created by the charges is in favour of the electron transfer from the reduced POM to $Ag^+$. Nevertheless, previous studies showed that the redox potential of the (silver ion/silver atom) couple is always lowered by ligands [31–35], but in those cases, the ligand was not the reducing species. We also cannot exclude the possible reduction of $Ag^+$ in the complex by an excited reduced POM, since it is known that the excited state of a redox reagent is a better reductant than the ground state. On the other hand, the reduction process can be initiated by the alcohol radical produced upon the photoreduction of the POM, the mechanism involving a complexation step as proposed in radiolysis experiments [30,36] according to reactions 6-7.

$$(CH_3)_2C^{\bullet}OH + Ag^+ \rightarrow [Ag(CH_3)_2C^{\bullet}OH]^+ \quad (6)$$

$$[Ag(CH_3)_2C^{\bullet}OH]^+ + Ag^+ \rightarrow Ag_2^+ + (CH_3)_2CO + H^+ \quad (7)$$

Association and coalescence reactions of the $Ag^+$ ions and initial silver clusters (reactions 8–10) lead then to the formation of silver particles.

$$Ag^0 + Ag^+ \rightarrow Ag_2^+ \quad (8)$$

$$2Ag_2^+ \rightarrow Ag_4^{2+} \quad (9)$$

$$Ag_m^{x+} + Ag_p^{y+} \rightarrow Ag_{(m+p)}^{(x+y)+} \quad (10)$$

Furthermore, as the redox potential of the silver clusters, $E^0(Ag_n^+/Ag_n)$ increases with the nuclearity $n$ [37], for clusters of nuclearity superior to 4 in the case of uncomplexed silver, the direct reduction of the $Ag_n^+$ clusters by the reduced POM or the alcohol radical become thermodynamically favourable. However, the POM may act as a ligand for the silver clusters and lowers the redox potentials of the metal particles even at rather high nuclearities. Strong influence of ligandation on the redox properties and coalescence rate have already been reported for silver complexes in water [27,31–35], in particular in the case of $CN^-$ [38]. The fact that the small formed particles are oxidised when the illumination is stopped indicates that their redox potentials are low enough for corrosion to occur, probably by $H_3O^+$ [39,40] and/or $(CH_3)_2CO$.

Fig. 5A and 6A present the absorption spectra recorded during the illumination of deaerated aqueous solution containing 0.13 mol $L^{-1}$ propan-2-ol, $6.4 \times 10^{-5}$ mol $L^{-1}$ $Ag_2SO_4$ and $8 \times 10^{-6}$ mol $L^{-1}$ $\alpha\beta\beta\alpha$-$Na_{17}[Co_4(H_2O)(OH)(P_2W_{15}O_{56})_2]\cdot 51H_2O\cdot 2NaCl$ or $\alpha\alpha\beta\alpha$-$Na_{16}[Co_4(H_2O)_2(P_2W_{15}O_{56})_2]\cdot 51H_2O$, respectively. In both cases, the reduction of the silver cations is evidenced by the apparition and growth of the absorption plasmon band of silver clusters around

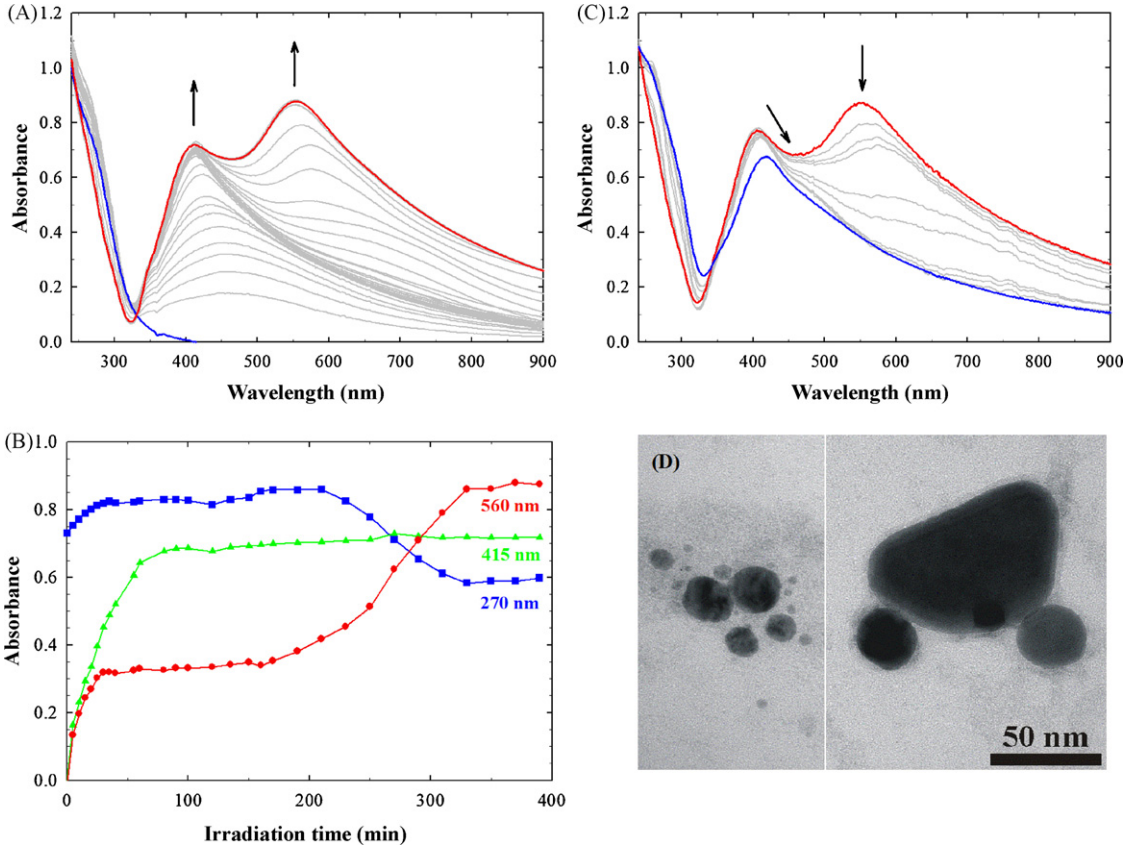


**Fig. 5.** (A) Change in the UV–vis absorption spectrum and (B) temporal evolution of the absorbance at three different wavelengths of a deaerated aqueous solution containing $8 \times 10^{-6}$ mol $L^{-1}$ $\alpha\beta\beta\alpha$-$Na_{17}[Co_4(H_2O)(OH)(P_2W_{15}O_{56})_2]\cdot 51H_2O\cdot 2NaCl$, $6.4 \times 10^{-5}$ mol $L^{-1}$ $Ag_2SO_4$ and 0.13 mol $L^{-1}$ propan-2-ol under illumination; (C) change in the UV–vis absorption spectrum of the same solution after the stop of the illumination and the opening of the cell to air; (D) TEM micrograph of the formed silver nanoparticles.

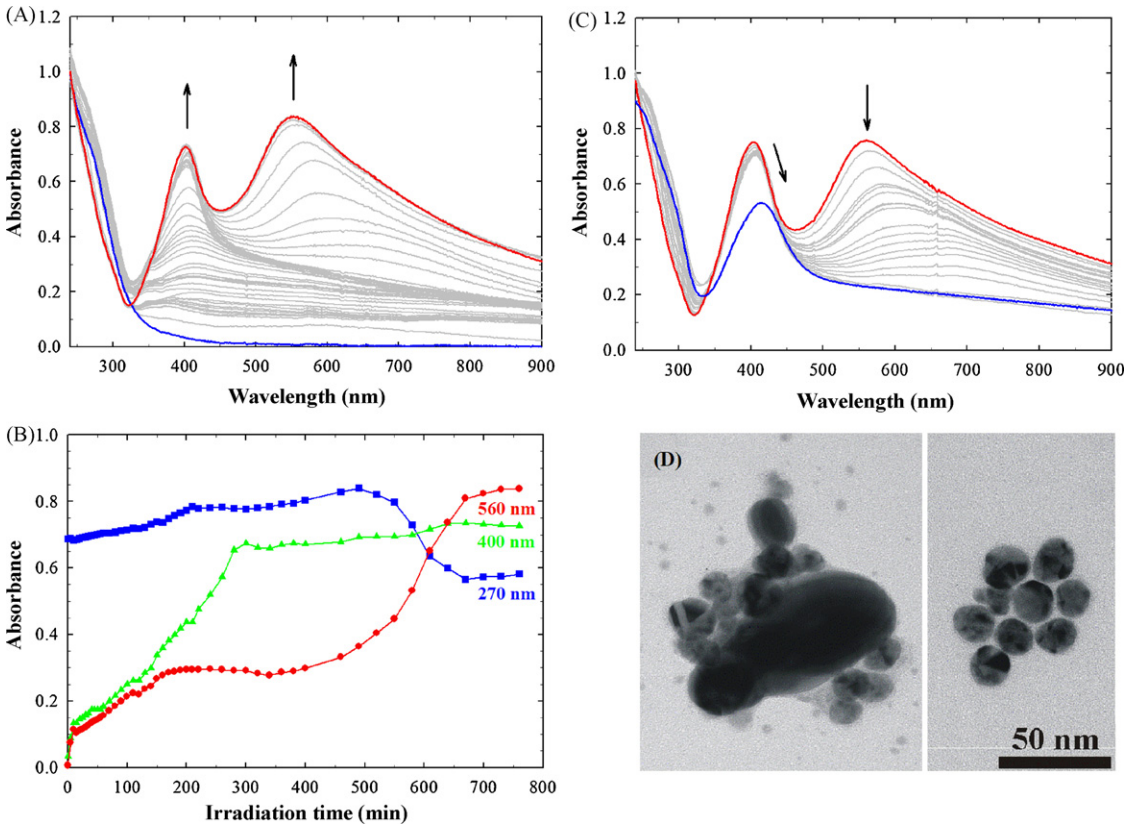


**Fig. 6.** (A) Change in the UV–vis absorption spectrum and (B) temporal evolution of the absorbance at three different wavelengths of a deaerated aqueous solution containing $8 \times 10^{-6}$ mol $L^{-1}$ αααα-$Na_{16}[Co_4(H_2O)_2(P_2W_{15}O_{56})_2]\cdot 51H_2O$, $6.4 \times 10^{-5}$ mol $L^{-1}$ $Ag_2SO_4$ and 0.13 mol $L^{-1}$ propan-2-ol under illumination; (C) change in the UV–vis absorption spectrum of the same solution after the stop of the illumination and the opening of the cell to air; (D) TEM micrograph of the formed silver nanoparticles.

400 nm. After 350 and 700 min of light exposure for ββ- and αβ-$\{Co_4P_4W_{30}\}$, respectively, the UV–vis spectra do not evolve any more what indicates the end of the reactions and the total reduction of $Ag^+$ into $Ag_n$ clusters. Compared to α-$[P_2W_{18}O_{62}]^{6-}$, in the case of ββ-$\{Co_4P_4W_{30}\}$, the plasmon band is less symmetric with a long tail in the low energy side and the molar extinction coefficient per $Ag^0$ atom at the peak maximum (412 nm) is much smaller (5400 $dm^3$ $mol^{-1}$ $cm^{-1}$). These spectral features indicate larger particles with less spherical shapes and/or a heterogeneous size distribution. Considering αβ-$\{Co_4P_4W_{30}\}$, the plasmon band shape appears intermediate between the two preceding ones; the spectrum presents a more defined and symmetric peak at 401 nm than the one obtained with ββ-$\{Co_4P_4W_{30}\}$ but with a similar molar extinction coefficient per $Ag^0$ atom and it also shows a very broad absorption in the whole visible domain. That suggests either elongated particles or the presence of two populations, small spherical nanoparticles on the one hand and quite large particles on the other hand.

The time evolution of the absorbencies at different wavelengths is given in Fig. 5B and 6B. For both $\{Co_4P_4W_{30}\}$, a jump of the absorbance in the visible range is observed at the beginning of the illumination (<5 min) indicating the quasi-instantaneous production of silver clusters. Such fast reactions may be related to the existence of POM-$Ag^+$ complexes in the solution, as suggested by the increase in the O–W CT absorption band upon addition of $Ag^+$. Then, the absorbencies near 400 and 560 nm go on rising regularly showing the formation of small $Ag_n$ clusters, then the absorbance at 400 nm continues to rise while the absorbance at 560 nm remains constant indicating the $Ag^+$ reduction processes and the formation of nanoparticles. After 80 and 300 min of illumination for ββ- and αβ-$\{Co_4P_4W_{30}\}$, respectively, the absorbance near 400 nm reaches a plateau indicating the total reduction of silver, whereas the absorbance at 560 nm increases and that at 270 nm concomitantly decreases showing the formation of reduced POM. Thus, we can estimate the average rate of $Ag^+$ reduction to be $1.6 \times 10^{-6}$ and $4.3 \times 10^{-7}$ mol $L^{-1}$ $min^{-1}$ for ββ- and αβ-$\{Co_4P_4W_{30}\}$, respectively. These values clearly show the influence of the POM structure on the kinetics of the photocatalysis, the symmetric isomer appearing more efficient than the asymmetric one.

For both $\{Co_4P_4W_{30}\}$ isomers, when the cell is opened to air, the absorption band around 550 nm disappears quickly showing the complete oxidation of the reduced POM, while the plasmon band decreases slightly and shifts to longer wavelengths indicating a weak oxidation and coalescence of the smallest clusters and the presence of stable silver nanoparticles (Fig. 5C and 6C). No precipitation is observed.

The TEM micrographs (Fig. 5D and 6D) confirm the formation of the silver particles upon illumination of deaerated aqueous solution containing propan-2-ol, $\{Co_4P_4W_{30}\}$ and $Ag^+$. The produced silver nanoparticles are quite inhomogeneous in size, between 10 and 100 nm; most of them are spherical but a few present triangular, elongated or bent shapes. Nevertheless, the obtained particles are stable against aggregation, what may be attributed to a stabilizing role of POM. Indeed, the colloidal solution contains no other potential stabilizing agent but POM. From radiolytic studies [41,42], it is known that $SO_4^{2-}$ ions do not stabilize the silver aggregates but accelerate both the formation of the clusters and their conversion to larger particles. So, the volume of $\{Co_4P_4W_{30}\}$ (with a length of ca. 20 Å and a width of ca. 10 Å) and its (16-) negative charge could account for the prevention of agglomeration of the metal particles, as for other POM [6,43–45].

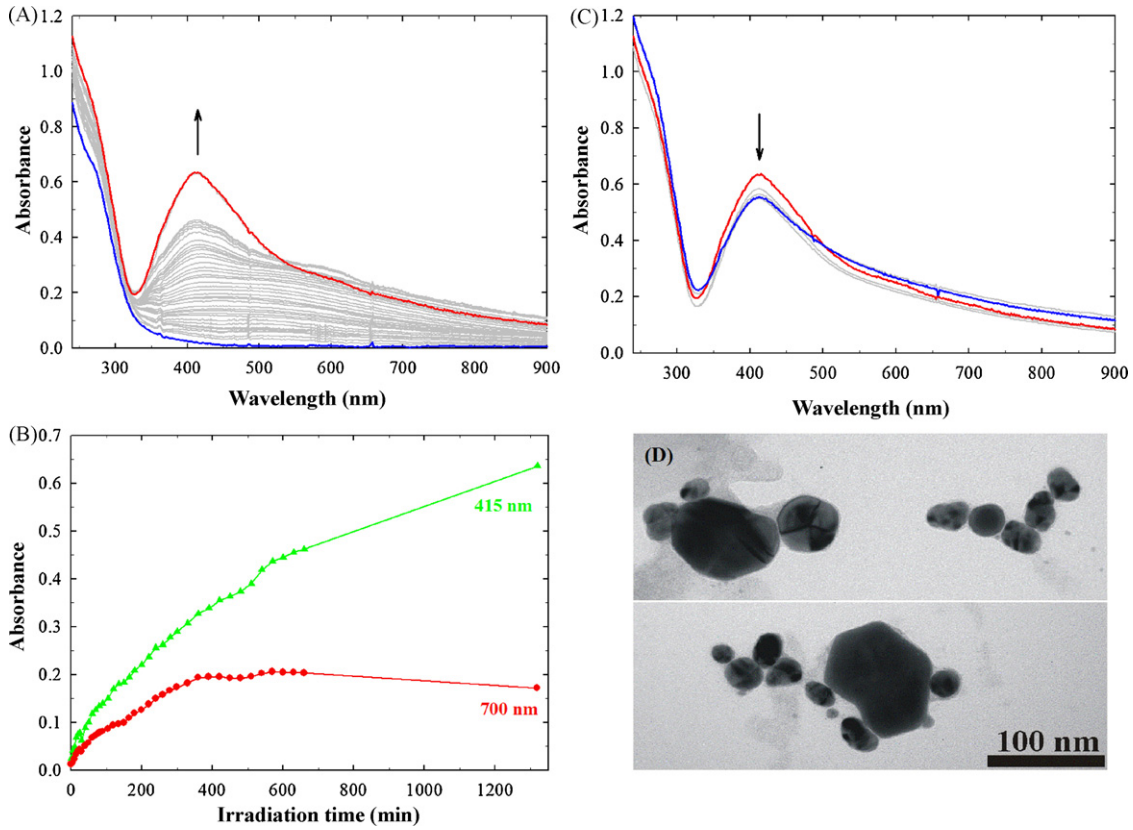


**Fig. 7.** (A) Change in the UV–vis absorption spectrum and (B) temporal evolution of the absorbance at two different wavelengths of an aerated aqueous solution containing $8 \times 10^{-6}$ mol $L^{-1}$ αββα-$Na_{17}[Co_4(H_2O)(OH)(P_2W_{15}O_{56})_2]\cdot 51H_2O\cdot 2NaCl$, $6.4 \times 10^{-5}$ mol $L^{-1}$ $Ag_2SO_4$ and 0.13 mol $L^{-1}$ propan-2-ol under illumination; (C) change in the UV–vis absorption spectrum of the same solution after the stop of the illumination; (D) TEM micrograph of the formed silver nanoparticles.

Those results show the photocatalytic activity of both $\{Co_4P_4W_{30}\}$ isomers toward the reduction of $Ag^+$ ions in the presence of propan-2-ol, although the thermodynamics do not seem favourable. We may suggest the same explanations as those proposed for α-$[P_2W_{18}O_{62}]^{6-}$, i.e., complexation between POM and $Ag^+$ and/or reduction via the alcohol radical for the initial reduction mechanism. In contrast to α-$[P_2W_{18}O_{62}]^{6-}$, the particles formed with both $\{Co_4P_4W_{30}\}$ are large and stable. The charge of the POM and the association of $Ag^+$ with POM may account for that difference between the sizes of the particles. If a larger number of $Ag^+$ is associated with $\{Co_4P_4W_{30}\}$ compared to α-$[P_2W_{18}O_{62}]^{6-}$, initially there will be fewer nuclei for the cluster growth and so, fewer but larger particles will be generated. Whereas the size of the particles may be related to the charge of the POM, it is difficult to explain how the symmetry of the $\{Co_4P_4W_{30}\}$ complexes affects the rate of silver reduction and slightly the shape and size of the formed particles. It is highly probable that the symmetry effect is related to different electronic distributions on the POM and/or geometrical effects modifying $Ag^+$ approaches and $Ag^0$ aggregation.

### 3.2.2. Photoreduction in the presence of dioxygen

For application purposes, constraints must be limited and, air conditions are preferred. So, we have tested the photocatalytic activity in the presence of dioxygen of ββ-$\{Co_4P_4W_{30}\}$, which has given the best results in anaerobic conditions.

Fig. 7A present the absorption spectra recorded during the illumination of aerated aqueous solution containing 0.13 mol $L^{-1}$ propan-2-ol, $8 \times 10^{-6}$ mol $L^{-1}$ αββα-$Na_{17}[Co_4(H_2O)(OH)(P_2W_{15}O_{56})_2]\cdot 51H_2O\cdot 2NaCl$ and $6.4 \times 10^{-5}$ mol $L^{-1}$ $Ag_2SO_4$. The reduction of the silver cations is evidenced by the apparition and growth of the absorption plasmon band of silver clusters around 400 nm. But, as the concentrations are the same as those previously used in deaerated condition, it is clear that the reduction processes are slowed down by at least a factor three since after 22 h of illumination the reduction is maybe not completed (Fig. 7B). Moreover, the shape of the absorption plasmon band is not so well defined and its intensity is smaller indicating large particles with a broad distribution in size as confirmed by TEM images (Fig. 7D). After the stop of the illumination, the formed nanoparticles

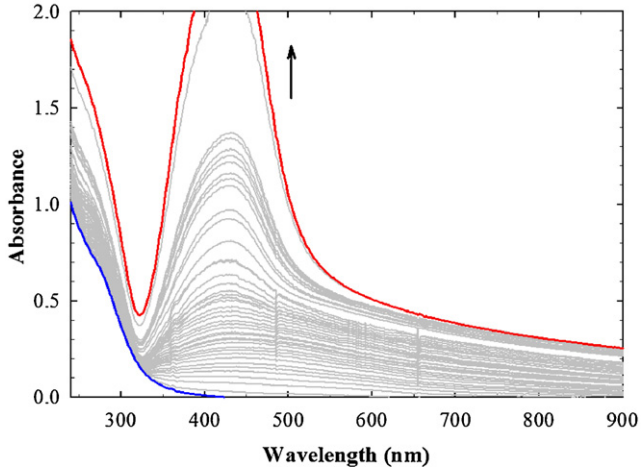


**Fig. 8.** Change in the UV–vis absorption spectrum of an aerated aqueous solution containing $8 \times 10^{-6}$ mol $L^{-1}$ αββα-$Na_{17}[Co_4(H_2O)(OH)(P_2W_{15}O_{56})_2]\cdot 51H_2O\cdot 2NaCl$, $4 \times 10^{-4}$ mol $L^{-1}$ $Ag_2SO_4$ and 0.13 mol $L^{-1}$ propan-2-ol under illumination.

aggregate in larger particles as shown by the small decrease in the plasmon band and the increase in the absorbencies below 350 nm and above 550 nm due to light scattering (Fig. 7C).

The slowing down of the reduction processes in the presence of dioxygen is easily explained by the competitive reactions of $O_2$ with the reduced POM and the alcohol radical leading to strong oxidizing agents ($O_2^{\bullet -}$, $HO_2^{\bullet}$, $H_2O_2$) [24,46]. In addition, the initial $Ag^0$ atoms and $Ag_n$ clusters can also be oxidised, hence the number of nucleation centres is diminished and the growth of large particles is favoured.

Fig. 8 illustrates the effect of $Ag^+$ concentration. When silver ions are in large excess compared to $\{Co_4P_4W_{30}\}$ (100 equivalents instead of 16), illumination of aerated solution containing propan-2-ol, $\{Co_4P_4W_{30}\}$ and $Ag^+$ gives large nanoparticles. But, as the absorbance of the plasmon band becomes too high ($A > 2$), it was not possible to determine the end of the reduction reaction.

## 4. Conclusion

The photocatalytic reduction of $Ag^I_2SO_4$ in deaerated aqueous solutions is observed in the presence of $\alpha$-$[P_2W_{18}O_{62}]^{6-}$ or $\{Co_4P_4W_{30}\}$ as photocatalyst and an organic substrate (propan-2-ol) as sacrificial electron donor. The direct photochemical excitation of the POM in the presence of propan-2-ol leads to its reduction. That photoreduction step induces electron transfer to $Ag^+$ ions to give $Ag^0$ metal atoms which form $Ag_n$ colloidal metal nanoparticles. In the case of $\alpha$-$[P_2W_{18}O_{62}]^{6-}$, the formed nanoparticles are small and not stable without illumination, while in the case of $\{Co_4P_4W_{30}\}$, the produced $Ag_n$ particles are large, almost spherical, stable without illumination in air conditions, and stable against aggregation because of the stabilizing role of POM. So, the charge and size of the polyoxometalate seem to have an influence on the size and stability of the formed silver particles. Moreover, the structure of the polyoxometalate also affects the kinetics of the reduction processes, the reduction being faster with the symmetric $\beta\beta$-$\{Co_4P_4W_{30}\}$ isomer than with the asymmetric $\alpha\beta$-$\{Co_4P_4W_{30}\}$ isomer. Experiments with other $\{M_4P_4W_{30}\}$ are in progress to study the effects of the central metal M of the POM on the kinetics of the reduction processes as well as on the size and stability of the formed nanoparticles.

At last, results with aerated solutions have showed that photocatalysis can also be effective under air conditions, what is promising for application purposes. Indeed, silver has been chosen as a model system for metal reduction, but the process could be applied in water depollution for reduction and recovery of valuable or toxic metals that could also be combined with the degradation of organic pollutants (sacrificial donor) as already proposed [11].

## Acknowledgment

This work was supported by the ANR agency, project no.: JC05_52437, NCPPOM. The authors thank P. Beaunier, Laboratoire de Réactivité de Surface, UMR 7609 CNRS-Université Paris VI (France) for the TEM observations.

## References

[1] M.T. Pope (Ed.), Heteropoly and Isopoly Oxometalates, Springer-Verlag, Berlin, 1983.
[2] C.L. Hill (Guest Ed.), Chem. Rev. 98 (1998) 1–389.
[3] L.E. Briand, G.T. Baronetti, H.J. Thomas, Appl. Catal. A: Gen. 256 (2003) 37–50.
[4] A. Troupis, A. Hiskia, E. Papaconstantinou, N. J. Chem. 25 (2001) 361–363.
[5] A. Troupis, A. Hiskia, E. Papaconstantinou, Environ. Sci. Technol. 36 (2002) 5355–5362.
[6] A. Troupis, A. Hiskia, E. Papaconstantinou, Angew. Chem. Int. Ed. 41 (2002) 1911–1914.
[7] A. Troupis, A. Hiskia, E. Papaconstantinou, Appl. Catal. B: Environ. 42 (2003) 305–315.
[8] A. Troupis, A. Hiskia, E. Papaconstantinou, Appl. Catal. B: Environ. 52 (2004) 41–48.
[9] E. Gkika, A. Troupis, A. Hiskia, E. Papaconstantinou, Environ. Sci. Technol. 39 (2005) 4242–4248.
[10] E. Gkika, A. Troupis, A. Hiskia, E. Papaconstantinou, Appl. Catal. B: Environ. 62 (2006) 28–34.
[11] A. Troupis, E. Gkika, A. Hiskia, E. Papaconstantinou, C. R. Chim. 9 (2006) 851–857.
[12] M.D. Ward, J.F. Brazdil, R.K. Grasselli, J. Phys. Chem. 88 (1984) 4210–4213.
[13] A. Ioannidis, E. Papaconstantinou, Inorg. Chem. 24 (1985) 439–441.
[14] C.L. Hill, D.A. Bouchard, J. Am. Chem. Soc. 107 (1985) 5148–5157.
[15] R. Thouvenot, M. Fournier, R. Franck, C. Rocchiccioli-Deltcheff, Inorg. Chem. 23 (1984) 598–605.
[16] L. Ruhlmann, L. Nadjo, J. Canny, R. Contant, R. Thouvenot, Eur. J. Inorg. Chem. (2002) 975–986.
[17] R. Constant, Inorg. Synth. 27 (1990) 104–109.
[18] L. Ruhlmann, C. Costa-Coquelard, J. Canny, R. Thouvenot, Eur. J. Inorg. Chem. (2007) 1493–1500.
[19] E. Papaconstantinou, Chem. Soc. Rev. 18 (1989).
[20] E. Papaconstantinou, M.T. Pope, Inorg. Chem. 9 (1970) 667–669.
[21] E. Papaconstantinou, D. Dimotikali, A. Politou, Inorg. Chim. Acta 43 (1980) 155–158.
[22] T. Yamase, N. Takabayashi, M. Kaji, J. Chem. Soc., Dalton Trans. (1984) 793–799.
[23] M.A. Fox, R. Cardona, E. Gaillard, J. Am. Chem. Soc. 109 (1987) 6347–6354.
[24] A. Hiskia, E. Papaconstantinou, Inorg. Chem. 31 (1992) 163–167.
[25] I.A. Weinstock, Chem. Rev. 98 (1998) 113–170.
[26] A. Henglein, R. Tausch-treml, J. Colloid Interf. Sci. 80 (1981) 84–93.
[27] S. Remita, M. Mostafavi, M.O. Delcourt, N. J. Chem. 18 (1994) 581–588.
[28] M. Mostafavi, J. Belloni, Recent Res. Dev. Phys. Chem. 1 (1997) 459–474.
[29] M.T. Pope, E. Papaconstantinou, Inorg. Chem. 6 (1967) 1147–1152.
[30] A. Henglein, Ber. Bunsenges. Phys. Chem. 81 (1977) 556–561.
[31] S. Remita, P. Archirel, M. Mostafavi, J. Phys. Chem. 99 (1995) 13198–13202.
[32] S. Remita, M. Mostafavi, M.O. Delcourt, J. Phys. Chem. 100 (1996) 10187–10193.
[33] I. Texier, S. Remita, P. Archirel, M. Mostafavi, J. Phys. Chem. 100 (1996) 12472–12476.
[34] I. Texier, M. Mostafavi, Radiat. Phys. Chem. 49 (1997) 459–464.
[35] I. Lampre, P. Pernot, M. Mostafavi, J. Phys. Chem. B 104 (2000) 6233–6239.
[36] R. Tausch-Treml, A. Henglein, J. Lilie, Ber. Bunsenges. Phys. Chem. 82 (1978) 1335–1343.
[37] J. Belloni, J. Amblard, J.L. Marignier, M. Mostafavi, in: H. Haberland (Ed.), Clusters of Atoms and Molecules, vol. II, Springer-Verlag, Berlin, 1994, pp. 290–311.
[38] C. de Cointet, M. Mostafavi, J. Khatouri, J. Belloni, J. Phys. Chem. B 101 (1997) 3512–3516.
[39] O. Platzer, J. Amblard, J.L. Marignier, J. Belloni, J. Phys. Chem. 96 (1992) 2334–2340.
[40] J. Amblard, O. Platzer, J. Ridard, J. Belloni, J. Phys. Chem. 96 (1992) 2341–2344.
[41] P. Mulvaney, A. Henglein, Chem. Phys. Lett. 168 (1990) 391–394.
[42] B.G. Ershov, E. Janata, A. Henglein, J. Phys. Chem. 97 (1993) 339–343.
[43] Y. Lin, R.G. Finke, J. Am. Chem. Soc. 116 (1994) 8335–8353.
[44] B. Keita, G. Zhang, A. Dolbecq, P. Mialane, F. Sécheresse, F. Miserque, L. Nadjo, J. Phys. Chem. C 111 (2007) 8145–8148.
[45] G. Zhang, B. Keita, A. Dolbecq, P. Mialane, F. Sécheresse, F. Miserque, L. Nadjo, Chem. Mater. 19 (2007) 5821–5823.
[46] Y.V. Geletii, C.L. Hill, R.H. Atalla, I.A. Weinstock, J. Am. Chem. Soc. 128 (2006) 17033–17042.